ELSEVIER

Journal of Nuclear Materials 266–269 (1999) 1172–1179

journal of nuclear materials

Operating window for high divertor radiation in ITER

H.D. Pacher [a,*], A.S. Kukushkin [b], D.P. Coster [c], A. Loarte [a], G. Janeschitz [b], D. Reiter [d], R. Schneider [c]

[a] *The NET Team, c/o Max-Planck-Inst. Plasmaphysik, Boltzmannstr. 2, 85748, Garching, Germany*
[b] *ITER Joint Central Team, Garching JWS, Garching, Germany*
[c] *Max-Planck Institut für Plasmaphysik, Garching, Germany*
[d] *FZ Jülich, Jülich, Germany*

Abstract

The operating parameters of the ITER divertor are varied around the partially attached operating point of Refs. [A.S. Kukushkin et al., Berchtesgaden, 1997; A.S. Kukushkin et al., Contributions to Plasma Physics 38 (1998) 20], to obtain an operating window with low heat load, acceptable He pumping and high divertor radiation. Lower heat diffusivities lead to higher heat loads which can be compensated by somewhat lower input power. The divertor geometry is varied: longer domes lead to higher heat loads, whereas the case without dome exhibits poorer helium pumping. Shorter divertor length cases show higher heat load and little change in helium pumping.

Keywords: 2D fluid code; 2D modelling; B2/EIRENE; ITER; Divertor modelling; Divertor target; Impurity radiation; Target plate; Power exhaust; Power flux; Helium exhaust

1. Introduction

The operating window of the ITER divertor [1], in divertor physics terms, is determined by the requirement that the power load on the divertor target plates not exceed 10 MW/m^2 and the helium ash be pumped at the rate of 2 Pa-m^3/s, for 1.5 GW fusion power and 200 MW incident on the scrape-off layer (SOL). Further constraints arise from matching to the core plasma: the Z_{eff} at the edge must not exceed 1.8 and the edge density (at the separatrix) must match the core density, i.e., be in the range $3 - 4 \times 10^{19}$ m^{-3}, the neutral reflux to the main plasma chamber should be small and the power transported across the separatrix should be higher than the L-H threshold (little radiation in the edge region of the core plasma). These requirements can be met if the plasma is in a partially attached state [2,3]. An operational point for ITER using Ne seeding to reduce the power load was given in [4] and initial assessments using radiation from both neon and the carbon generated by sputtering at the divertor plates was given in Refs. [5,6].

This paper describes an assessment of the operational window of the ITER divertor using B2-EIRENE, treating issues related both to the operational parameters (reduced radial transport, SOL power reduction) and the divertor geometry (length and absence of dome structure, length of divertor from X-point to target).

2. Simulation model

The B2-EIRENE code package [7,8] (full multi-fluid treatment of impurities together with a Monte-Carlo model for neutrals) has been used in the calculations. The plasma is assumed to consist of D, He, C, and Ne ions and neutrals, including D_2 (in these calculations, D represents both D and T isotopes). The cross-field diffusivities have been assumed to be constant. The input power Q_{sep} is uniformly distributed over the core-edge interface (CEI). Additional gas puffing at a rate of 10^{22} s^{-1} (molecules) is included in the model, and pumping from the private flux region (PFR) is simulated by

* Corresponding author. Tel.: +49 89 3299 4293; fax: +49 89 3299 4312; e-mail: pacherh@ipp-garching.mpg.de

0022-3115/99/$ – see front matter
PII: S0022-3115(98)00567-4

specifying the albedo A_p at the bottom of the PFR for all recycling species. Carbon is assumed to be sputtered from the targets and absorbed on all the surfaces, with zero net flux across the CEI (steady state). Realistic physical sputtering is included and a simplified model is used for chemical sputtering: carbon atoms with 1 eV energy (rather than the actual hydrocarbon molecules) are emitted at a constant sputtering yield $Y_{Ch} = 0.01$. Seeded neon is introduced by specifying its concentration at the CEI as a boundary condition. The electron density at the outer separatrix in the midplane, n_s, and the average Z_{eff} at the CEI are selected as the matching parameters for the core plasma. The neon density at the CEI and the D particle content have been varied in order to obtain scans in Z_{eff} and n_s, and each of the studies described below is carried out in terms of such scans. The following are taken as the standard conditions, similar to those of Ref. [6].

The density of hydrogenic species is specified to be constant, n_c at the CEI. The intrinsic helium concentration is set to 10% at the CEI. Q_{sep} is 200 MW presupposing ~100 MW radiation from the core [1], and $A_p = 0.95$. The cross-field diffusivities are $\chi_\perp = 1$ m^2/s, $D_\perp = 0.3$ m^2/s, yielding e-folding lengths of the radial profiles of the temperature and density in the midplane around $\lambda_T \approx 1.5$ cm, $\lambda_n \approx 2.5$ cm.

More comprehensive modelling of the processes involving the hydrogenic molecules is being started. Standalone runs were done with EIRENE including elastic collisions of neutral particles with plasma ions, vibrational excitation of the molecules, and ion conversion (these processes are neglected in all the other calculations presented here). The first, very preliminary results involving, in particular, treatment of vibrationally excited molecules as separate species indicate that (a) molecule-assisted recombination [9] may not be very important for the ITER conditions, contributing only 10–20% to the recombination, (b) elastic collisions and vibrational excitation can significantly increase the role of molecules in the energy and momentum balance of the ITER divertor plasma, and (c) a collisional-radiative model (e.g. [9]) is not well applicable to the distribution of molecules in vibrationally excited states. Work is continuing towards including these effects in the coupled code.

Several different studies have been undertaken in order to explore further the operational space of the ITER divertor and to see a possible effect of some modifications of divertor geometry. A wider range of Z_{eff} and n_s than in [6] has been covered by the calculations. Among other sensitivity studies, the cross-field diffusivities were reduced ($\chi_\perp = 0.5$ m^2/s, $D_\perp = 0.2$ m^2/s). In one series, this radial transport reduction was accompanied by a reduction of the input power by 50 MW in order to simulate enhanced radiation from the "mantle" [4]. First exploratory runs have also been done for the reduced particle throughput. In this case, the particle influx of deuterium at 3.1×10^{22} s^{-1} and helium at 5.4×10^{20} s^{-1} is specified at the CEI, in addition to the standard gas puff, and the density variation is achieved by varying A_p.

The divertor geometry is varied by changing the shape of the dome (the plasma-facing component just below the X-point in the PFR). Four different dome configurations [6] are studied in more detail to simulate a more slot-like divertor geometry (longer domes) and to determine the effect of simplifying the divertor geometry (removal of the dome).

The divertor geometry is further varied by shortening the divertor. We have selected two more divertor geometries, corresponding to a distance along the separatrix from the X-point to the target of approximately 3/4 and 1/2 the corresponding length for the standard case, and have kept the "wetted area" the same for the flux surfaces between the separatrix and the 2 cm surface (midplane values) for the outer divertor (the 4 cm surface for the inner divertor). This is intended to exclude the geometrical effect of the flux expansion near the X-point on the power load in the vicinity of the separatrix strike-points. For both design modification studies, the standard of the parameters has been used.

3. Variation of operation parameters

The peak heat load is given as a function of the upstream density n_s in Fig. 1 for the various operation parameters. For the standard case, it is seen that the

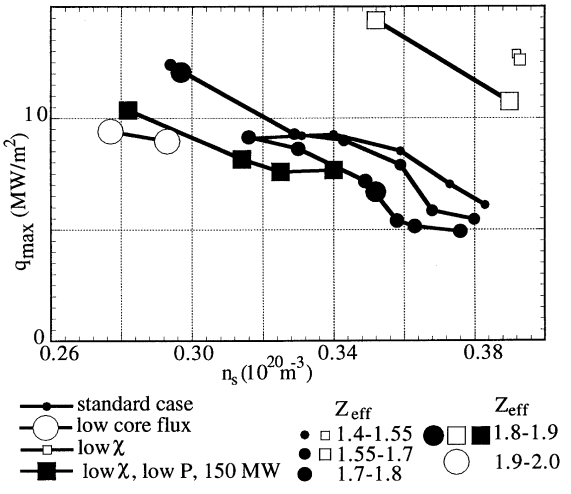

Fig. 1. Peak power load at the divertor target vs. upstream density n_s for "standard case" (solid circles), for lower χ and D (hollow squares), for simultaneous lower χ and D and lower SOL power (solid squares) and for lower throughput (hollow circles), all for reference divertor geometry. Various Z_{eff} (obtained by varying the neon fraction) are indicated by symbol size.

peak heat load varies strongly with n_s and less strongly when Z_{eff} is varied by varying the neon fraction, particularly at low n_s. The reason for the weak variation with Z_{eff} is seen in Fig. 2: the radiation fraction varies little with Z_{eff}, staying between 55% and 65% of the SOL power. The increase in neon radiation is largely offset by a decrease in carbon radiation (Fig. 2) corresponding to a decrease in the carbon content.

Lower $\chi_\perp$ and $D_\perp$ (see above) lead to much higher heat loads (Fig. 1). When the input power is reduced by 25%, the low transport cases yield peak heat loads which are even below those of the standard case but with narrower profiles, and the radiation fraction is the same for the 200 MW standard and the 150 MW low transport cases.

For the standard case, the helium partial pressure (Fig. 3) at low n_s is 0.025 Pa (for 2 Pa-m^3/s at $S = 170 m^3$/s, 0.012 Pa would be required), rising as n_s increases. The DT throughput at low n_s is 200 Pa-m^3/s, and the assumed A_p corresponds to a pumping speed of about 140 m^3/s. In the present calculation (Monte Carlo, neglecting neutral-neutral collisions in the PFR and elastic collisions between neutral He and D or T ions), at constant A_p, the pumping speed for He is not necessarily the same as for DT, and the value for He throughput is difficult to determine in the simulation (noise), so that further precise work (both in adjusting the code input and in the diagnostics) is required. The reduced throughput, reduced pumping case (at low n_s) has a lower helium pressure, a somewhat lower power load, but a higher Z_{eff} and a higher He fraction (13%) at the CEI than the standard case.

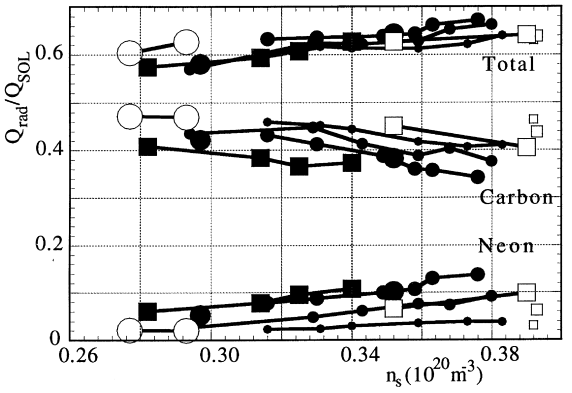

Fig. 2. Radiated power (summed over divertor, SOL, and edge region – the latter is <10 MW) normalised to SOL power for total radiation (impurities and neutrals), and carbon and neon separately vs. n_s for reference divertor geometry. Legend see Fig. 1.

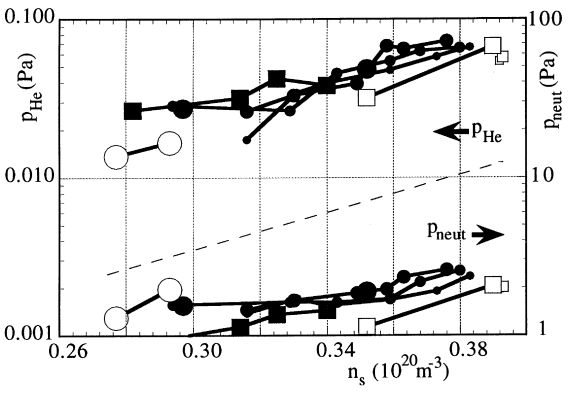

Fig. 3. Average helium partial pressure and total neutral pressure at plasma–PFR interface vs. n_s for reference divertor geometry. Legend see Fig. 1.

4. Variation of dome length

As the dome length is decreased from four times standard via standard toward no dome, the plasma parameters in the PFR just below the X-point evolve toward lower electron temperature (Fig. 4) and higher density. The ionization source moves toward the X-point, and neutrals fill the PFR just below X-point (Fig. 5), but are still stopped at the separatrix by the plasma. The neutral density beyond the separatrix remains much smaller than in the PFR even without the dome.

The standard dome has the best peak power load (Fig. 6), but the power load without dome is similar, as are the radial power load profiles. Longer domes have progressively more attached plasmas (higher T_e at the strike point) and have significantly higher peak power, by a factor 1.5, than the standard case and this cannot be compensated by increased Z_{eff} (Fig. 6).

When the dome is removed, the radiation in the core plasma (between the CEI and the separatrix) does not increase, and is low in all cases (<10 MW) so that edge cooling is not expected, nor is it seen on the edge temperature.

Radial density profiles at various poloidal positions show little effect of dome length, except for a local peaking which occurs for the case without dome only just outside the separatrix just above X-point, but there is no change in density on closed flux surfaces. There is no clear variation of neutral influx across the separatrix with dome length; it remains small (2×10^{21} s^{-1} compared to fueling of 10^{23} s^{-1}).

All the cases which have a dome have similar helium partial pressure (Fig. 7), but for the case without a dome P_{He} is lower by a factor 2.

In summary, an increase of the dome length from the standard length shows no difference in radial density profiles nor in helium pumping compared with the standard case, but is disadvantageous because it leads to

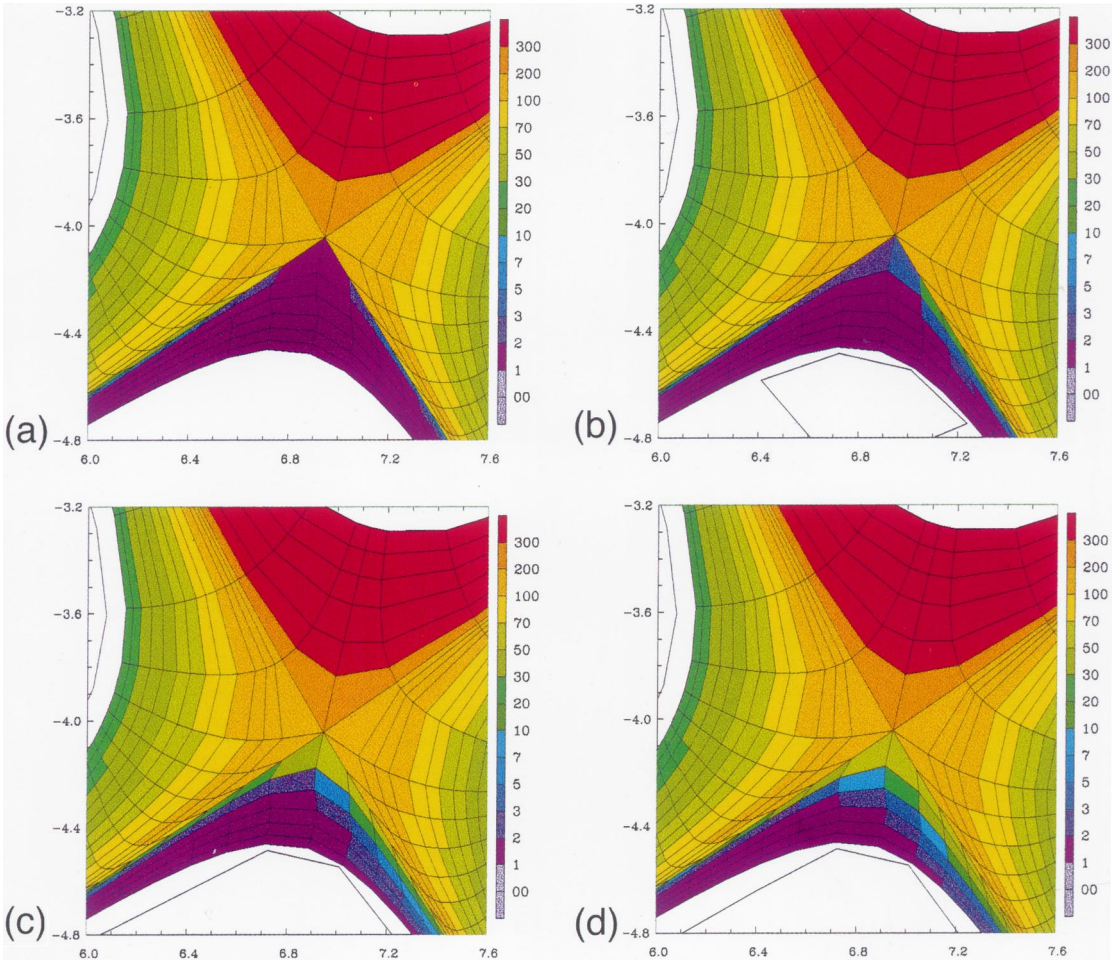

Fig. 4. Electron temperature (eV) in the vicinity of the X point without dome (a) standard dome (b) and longer domes (c,d).

higher power loading. Removal of the dome leads to no increase of the neutral penetration into the main plasma, no extensive cooling of the plasma edge, and no reduction of the plasma temperature at the separatrix. However, removal of the dome would have the disadvantage of reducing the helium pressure in the PFR by a factor of 2. The wider radial n_e profile with a local maximum outside the separatrix just above the X-point might affect confinement. Furthermore, removal of the dome would preclude use of a septum (not studied here) and reduce neutron shielding (to be quantified).

5. Variation of divertor length

As the divertor length is reduced from standard to 3/4 to 1/2, the temperature profile does not change strongly (Fig. 8) but the plasma in the shortest divertor is somewhat less detached. There is a clear shift of all impurities (Z_{eff} is shown in Fig. 8 as an indicator, but this is equally true for He, C, and Ne densities) from the outer divertor toward the inner divertor as the length is reduced. Possibly, this is due to the change of the angle between the target and the separatrix which was used to keep the wetted area constant as the flux expansion increased, see above. The ionization source is similar for all divertor lengths.

The peak power load is 1.5 times higher for the 1/2 length divertor than for the standard case (Fig. 9), but this can be reduced somewhat by increasing Z_{eff} (see 3/4 length case). Only a few cases have been calculated, so these results are preliminary pending a full n_s–Z_{eff} scan. The power load profile along the target for various divertor lengths (at varying angles) is somewhat narrower for shorter divertors, presumably because of less spreading in the shorter distance.

The radiation power is well distributed poloidally for all cases, but has a larger fraction close to the target for

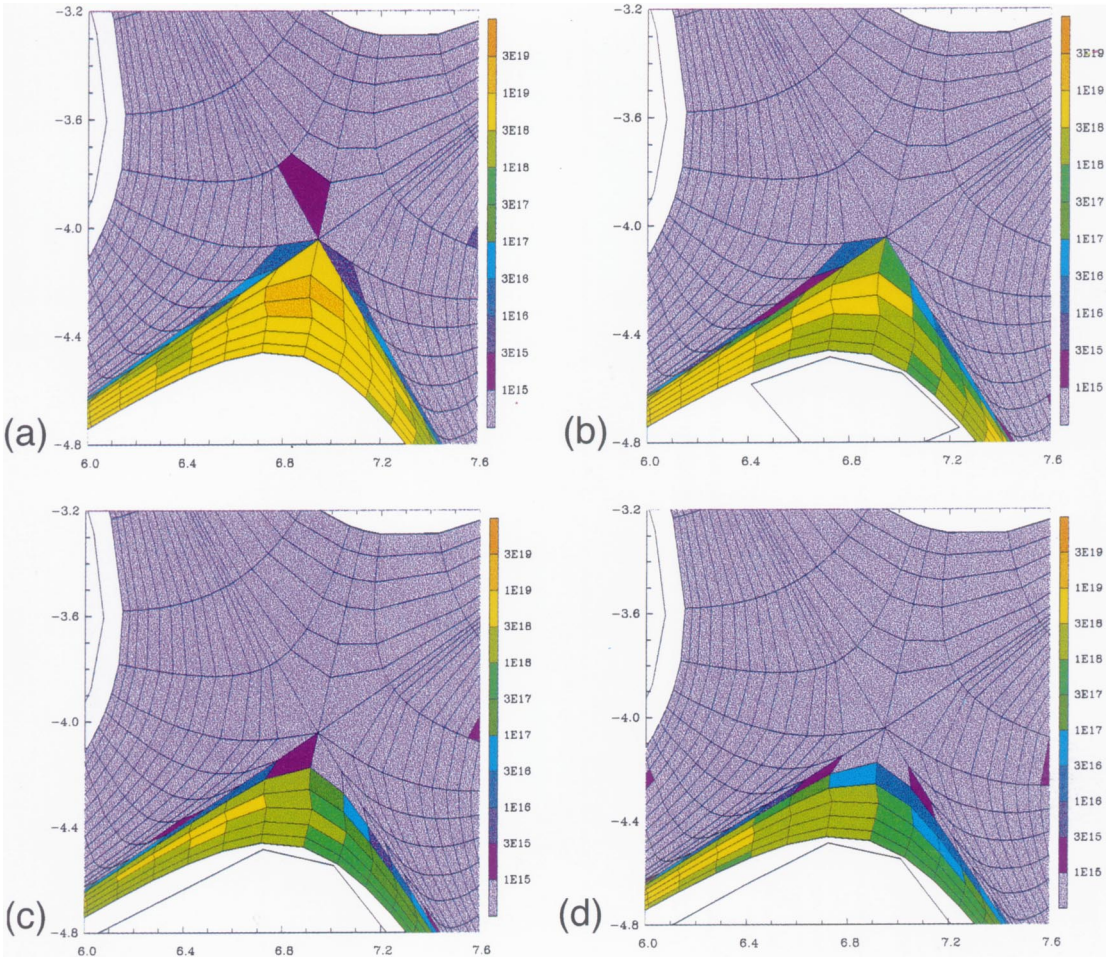

Fig. 5. Neutral density (m^3) in the vicinity of the X point without dome (a) standard dome (b) and longer domes (c,d).

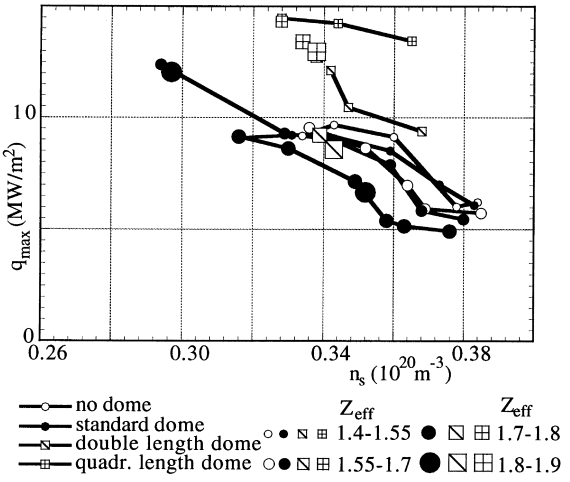

Fig. 6. Peak power load as in Fig. 1 but for three dome lengths and without dome.

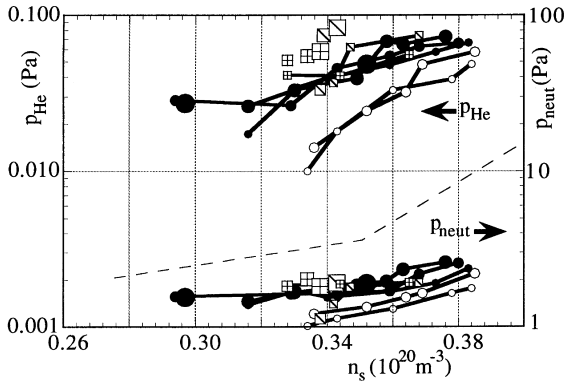

Fig. 7. Helium and total pressure as in as Fig. 3 but for three dome lengths and without dome. Legend as in Fig. 6.

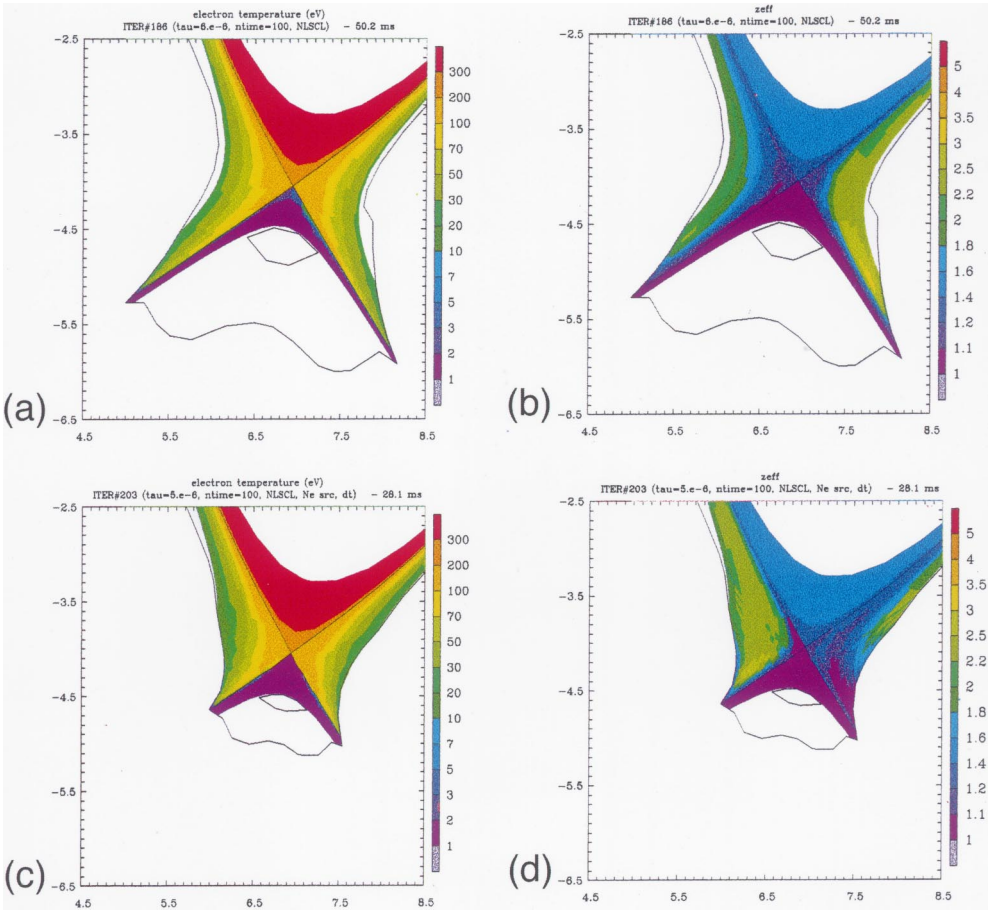

Fig. 8. Electron temperature in eV (a,c) and Z_{eff} (b,d) from the X-point to the targets for standard (a,b) and half-length (c,d) divertor.

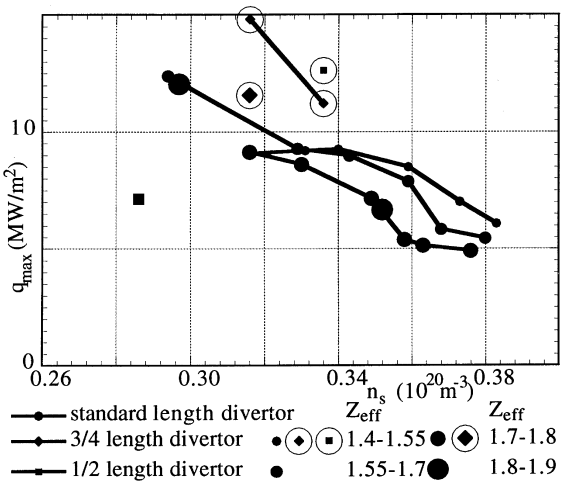

Fig. 9. Peak power as in Fig. 1 but for standard, three-quarter, and half-length divertors.

the short divertor. As shown in Fig. 10, 2/3 of the divertor radiation is in the vicinity of the target outboard and inboard for the shortest divertor, whereas for the standard divertor, these numbers are 1/3 inboard and 1/2 outboard, so the poloidal distribution for the standard divertor is better. For all cases, the radiation in the edge and SOL above the X-point (central panel of Fig. 10) is only a few MW. The radiation fraction is similar for all divertor lengths, but rises by a few percent for the shortest divertor, for which the carbon radiation fraction rises by 10%.

He pumping is similar for the 1/2 length and full length divertor (Fig. 11). The reduced value for the 3/4 length divertor may be due to the particular choice of target angle there.

In summary, results on the effect of divertor length are preliminary because only a few cases have been run and no higher density cases are available yet. Compared to the standard divertor, the peak power load is higher (50%) for the shorter divertor, the He pumping is similar, impurities congregate more at the inner target for

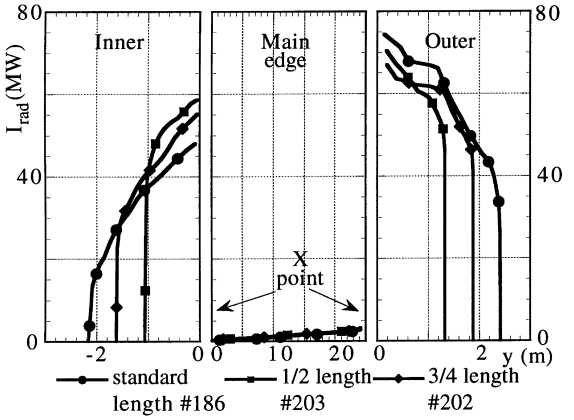

Fig. 10. Cumulative integral of radiation power density (already integrated radially) in poloidal direction vs. distance from target to X-point (inner divertor and PFR, left panel), from X-point to X-point (edge plasma and SOL, central panel) and from X-point to target (outer divertor and PFR, right panel), for standard, three-quarter, and half-length divertors.

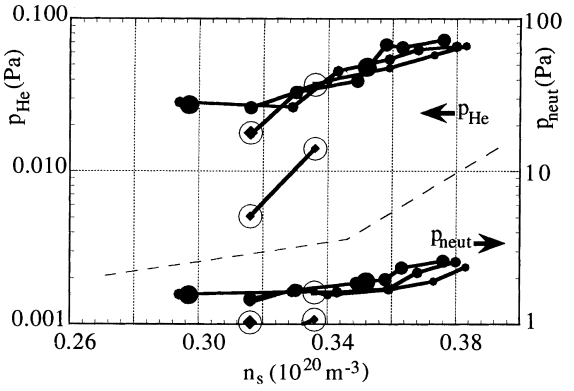

Fig. 11. Helium and total pressures as in Fig. 3 but for standard, three-quarter, and half-length divertors. Legend as in Fig. 9.

the shorter divertor, and the radiation is less well spread out poloidally.

6. Conclusions

As the operation parameters of the divertor are varied, lower transport coefficients (by a factor 2, $\chi_\perp = 0.5$ m^2/s, $D_\perp = 0.2$ m^2/s) and low n_s are found to lead to heat loads above 10 MW/m^2. These can be rendered manageable (below 10 MW/m^2 for n_s down to 3×10^{19} m^{-3} and Z_{eff} below 1.8) if the power incident on the SOL can be reduced by 25% to 150 MW, e.g. by edge radiation with an appropriate impurity. Lower DT throughput at the same n_s can be achieved by reducing pumping, but the margin in He pumping is reduced. A DT throughput lower than the standard case by a factor 2 is found for $n_s = 3 \times 10^{19}$ m^{-3} (only low n_s have been modeled so far) to lead to a helium concentration somewhat above 10%, higher than acceptable, at the core edge interface. Further investigations of DT and He throughput are required.

Increasing the dome length leads to higher peak power loads and higher densities for partial detachment and is therefore not recommended. Removal of the dome leads to neither significant cooling of the X-point region nor to increased neutral influx to the core. However, a local peak in the density just outside the separatrix near the X-point is found. Moreover, He pumping is degraded by a factor 2 when the dome is removed. For this and other reasons (improved shielding, possibility of installing a septum) it is preferable to retain the dome.

At the same Z_{eff} and n_s, halving the divertor length leads to an increase of peak heat load by a factor 1.5 for the configuration investigated (few runs have been carried out so far). Acceptable peak heat loads for this case at 200 MW are expected at Z_{eff} of 1.7–1.8 and n_s above 3.4×10^{19} m^{-3}. Helium pumping is affected relatively little. Further optimization of the calculations is required, particularly investigation of the effect of divertor plate angle (impurities move to the inner divertor in the present runs).

In conclusion, the ITER divertor can accommodate low $\chi_\perp$ and low n_s with a modest SOL power reduction and an acceptable operating window for heat load and He pumping. Modifications desirable for other reasons (shorter divertor, dome removal, reduced DT throughput) reduce this window.

Acknowledgements

This report is an account of work undertaken within the framework of the ITER EDA Agreement. The views and opinions expressed herein do not necessarily reflect those of the parties to the ITER Agreement, the IAEA or any agency thereof. Dissemination of the information in this paper is governed by the applicable terms of the ITER EDA Agreement.

References

[1] R. Parker et al., J. Nucl. Mater. 241–243 (1997) 1.
[2] G. Janeschitz, K. Borass, G. Federici et al., J. Nucl. Mater. 220–222 (1995) 73.
[3] A.S. Kukushkin, H.D. Pacher et al., J. Nucl. Mater. 241–243 (1997) 268.

[4] A.S. Kukushkin, H.D. Pacher et al., 16th IAEA Fusion Energy Conference, Montreal, 1996.
[5] A.S. Kukushkin, H.D. Pacher et al., Proc. 24th EPS Conf. Contr. Fusion and Plasma Physics, Berchtesgaden, 1997.
[6] A.S. Kukushkin, H.D. Pacher, D.P. Coster et al., Contr. Plasma Phys. 38 (1998) 20.
[7] D. Reiter, H. Kever, G.H. Wolf et al., Plasma Phys. Contr. Fusion 33 (1991) 1579.
[8] R. Schneider, D. Reiter, H.-P. Zehrfeld et al., J. Nucl. Mater. 196–198 (1992) 810.
[9] A.Yu. Pigarov, S.I. Krasheninnikov, Phys. Lett. A 222 (1996) 251.